Determination of the flow and activation energy of phosphorus desorption during annealing of an InP(001) substrate in an arsenic flux under molecular beam epitaxy conditions

© D.A. Kolosovsky, D.V. Dmitriev, S.A. Ponomarev, A.I. Toropov, K.S. Zhuravlev

Rzhanov Institute of Semiconductor Physics, Siberian Branch, Russian Academy of Sciences, 630090 Novosibirsk, Russia

E-mail: d.kolosovsky@isp.nsc.ru

Received March 2, 2022
Revised March 25, 2022
Accepted March 25, 2022

We report experimental study of phosphorus desorption from *epi-ready* InP(001) substrates during high-temperature annealing in an arsenic flux. InPAs solid solution and InAs islands are formed on the surface in the process of annealing. The original method is proposed to determine the amount of phosphorus atoms desorbing from the surface by determining the amount of arsenic atoms in the solid solution of InPAs and InAs islands. The flux of phosphorus desorbing from the surface increases from $1 \cdot 10^{-4}$ monolayer $\cdot$ cm$^{-2} \cdot$ s^{-1} at 500°C annealing temperature to $7.3 \cdot 10^{-4}$ monolayer $\cdot$ cm$^{-2} \cdot$ s^{-1}at 540°C. The activation energy of the phosphorus desorption process is 2.7 ± 0.2 eV.

Keywords: InP, annealing, desorption, activation energy.

DOI: 10.21883/SC.2022.07.54757.09

1. Introduction

Indium phosphide (InP) substrates are actively used in molecular beam epitaxy (MBE) and metal-organic vapor deposition (MOCVD) methods for the growth of heterostructure (HES) [1,2], since indium phosphide has a high carrier mobility charge, direct band gap and large radius of Bohr excitons [3,4], which makes indium phosphide the promising technological platform for the modern element base of microwave photonics [5]. The InP-based platform makes it possible to create completely monolithic integrated microwave photonic circuits, and HESs lattice matched with InP have excellent optical properties, allow to generate, amplify and detect light, modulate and control the light flux [6,7]. The HES growth process begins with the removal of the amorphous oxide layer of the substrate. It is usually removed by high temperature annealing in ultrahigh vacuum [8]. However, the temperature of complete removal of the oxide layer, which is ~ 500°C [9], is higher than the temperature of phosphorus desorption and formation of indium droplets, which is ~ 350°C [10,11]. Therefore, to prevent surface dissociation, InP substrates are annealed in a flux of phosphorus or arsenic [9].

Phosphorus is tried not to be used in the annealing process of substrates, since it is difficult to remove it from the growth chamber, and the presence of phosphorus in the growth chamber during HES growth results in its uncontrolled incorporation into epitaxial layers [12]. The incorporation of phosphorus into epitaxial layers results to the formation of quaternary interface layers with rough heterointerfaces [13]. Annealing in an arsenic flux is preferable, since arsenic is more easily removed from the growth chamber, and arsenic-based HESs have smoother heterointerfaces and make it possible to create devices with a wider operating temperature range [14].

However, during the annealing of InP in the flux of arsenic, the exchange interaction occurs between phosphorus and arsenic [15–17], as a result of which arsenic takes the place of phosphorus in the crystal lattice. When the arsenic flux interacts with atomically clean surface, phosphorus is completely replaced by arsenic in the near-surface layer of the substrate (1.3–2.6 bilayer) and strained InAs layers are formed [11]. The mechanisms of these processes are well studied and discussed earlier [18–20]. The flow of phosphorus desorbing from the surface and its activation energy were determined in the works [21–23]. The values of the activation energies are given in Table 1.

When an oxide layer is on the InP surface, annealing in an arsenic flux results in a different surface condition The process of exchange interaction becomes more complicated, the surface has more complex morphology and composition. Solid solution of InPAs with InAs islands is formed on the surface [24–27]. The composition of the solid solution and the density of islands depend on the annealing conditions. The fundamental reason for surface transformation is also the desorption of phosphorus from the surface. To construct

Table 1. Comparison of phosphorus desorption activation energies obtained by different research groups

Activation energy, eV	Reference
3.36	Lee et al. [21]
2.96	Kobayashi and Kobayashi [22]
2.4	Sun et al. [23]

a model of nucleation and understand the initial processes of HES growth in such a system, it is necessary to know the value of the desorbing from the surface phosphorus flow and its activation energy.

In this work, the method for determining the flow of phosphorus desorbing from the surface and its activation energy from data on the morphology and elemental composition of the InP(001) surface annealed in an arsenic flux, is proposed. The flow of phosphorus desorbing from the surface at typical InP annealing temperatures in arsenic and its activation energy are determined.

2. Method for determining the flow of desorbing phosphorus

Figure 1 shows the schematic representation of the *epi-ready* surface of an InP(001) substrate after high temperature annealing in an arsenic flux. The formation of an InAs island and an InPAs solid solution requires indium, phosphorus, and arsenic atoms. We will assume that the number of indium and arsenic atoms in InAs islands corresponds to 1 : 1. An amorphous oxide layer consisting of In_2O_3, $InPO_3$, $InPO_4$, $In(OH)_3$ and $In(PO_3)_3$ can be a source of indium atoms [28–31]. It can be seen that the oxide layer contains indium atoms, which can participate in the formation of a solid solution and islands. Also indium atoms can arrive at the surface from the InP substrate by breaking the bond with the fifth group atoms. Since the desorption coefficient of phosphorus is higher than that of arsenic by ~ 100 times [32,33] and, according to the SEKI thermodynamic model, the chemical reaction constant of InAs formation is greater than the chemical reaction constant of InP formation [34], then the breaking of the bond between indium atoms and phosphorus atoms is more probable than breaking the bond between indium atoms and arsenic atoms. After breaking the bond of indium atoms with phosphorus atoms, the latter desorb from the surface, while the former interact with arsenic, which comes to the surface of the substrate from the molecular source. Thus, it can be seen that if we determine the number of indium atoms in the InPAs solid solution and InAs islands, which arrived due to the breaking of the bond with phosphorus, one can determine the number of phosphorus atoms desorbing from the surface.

To exclude indium atoms coming from the oxide layer, we will consider the InPAs solid solution and InAs islands at two time points. The first time point is the moment of formation of the structure (4×2) in the diffraction pattern, which evidences of atomically clean surface of the substrate [35]. The formation of atomically clean surface indicates that all indium atoms from the oxide layer have been incorporated into the crystal structure. The second time point will be a two-minute exposure in the arsenic flux at the structure formation temperature (4×2), since 2 minutes is a typical transition time between the annealing process to the HES growth process. By determining the difference in the number of arsenic atoms in the InPAs solid solution and the InAs islands between these two time points, one can exclude the number of indium atoms, the source of which was the oxide layer.

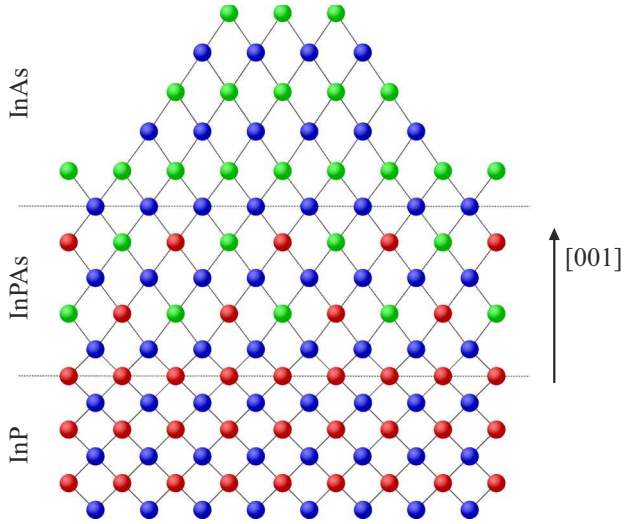

Figure 1. Schematic representation of the crystal lattice of the InP(001) substrate after high-temperature annealing in an arsenic flux. Indium — blue, phosphorus — red, arsenic — green. (A color version of the figure is provided in the online version of the paper).

3. Experimental technique

For research, InP(001) substrates by AXT were used. Samples were annealed in the growth chamber of Riber Compact 21T MBE system. The MBE system is equipped with infrared pyrometer „Ircon Modline Plus“ for *in situ* control of the substrate temperature. Preliminary calibration of the pyrometer readings was carried out according to the temperature of reconstruction transitions on the InP surface [36,37]. The temperature measurement error was 1%. The reflection high-energy electron diffraction (RHEED) system was used to *in situ* control processes on the substrate surface. The kSA 400 system by k-Space Associates was used to analyze the diffraction patterns. Arsenic flux F_{As} was varied by VAC 500.valved source. Arsenic flux data was taken with a special vacuum sensor, the „Bayard-Alpert JBA“ ionisation lamp. During measurements, the lamp was placed under the substrate, and after measurements it was removed into a special cavity in the growth chamber. The surface morphology of the studied samples was analyzed using a Bruker Multimode 8 atomic force microscope (AFM) and the Gwyddion software package.

The experimental samples were divided into two series. The annealing of samples of the first series was completed when the structure was obtained (4×2), the samples of second series were additionally exposed for 2 min in

Table 2. F_{As} and T_{sub} values at which the structure is formed (4×2) [24]

T_{sub} (°C)	F_{As}, Topp
500	$1.1 \cdot 10^{-5}$
520	$1.63 \cdot 10^{-5}$
540	$2.5 \cdot 10^{-5}$

Table 3. Values of the lattice constant of the solid solution InPAs and InAs [24]

T_{sub} (°C)	a_0, nm	
	InPAs	InAs
500	0.5894	0.60583
520	0.5930	
540	0.5946	

Table 4. The number of arsenic atoms in the InPAs solid solution and InAs islands

T_{sub} (°C)	N_{As}, $cm^{-2} \cdot nm^{-1}$		
	InPAs	InAs	
		$t = 0$ s	$t = 120$ s
500	$2.5 \cdot 10^{14}$	$5.8 \cdot 10^{12}$	$1.3 \cdot 10^{13}$
520	$6.5 \cdot 10^{14}$	$6.5 \cdot 10^{12}$	$2.5 \cdot 10^{13}$
540	$7.8 \cdot 10^{14}$	$1 \cdot 10^{13}$	$6.3 \cdot 10^{13}$

F_{As} at annealing temperature (T_{sub}) equal to the structure formation temperature (4×2), after which the annealing process was completed. Structure formation (4×2) was controlled by RHEED method. The substrate temperature during annealing changed at the rate of ~ 10°C/min. After annealing was completed, the samples were cooled in arsenic flux at the rate of ~ 50°C/min. The values of F_{As} at T_{sub}, at which the structures (4×2) are formed, are presented in Table 2. The choice of annealing temperatures of 500, 520, and 540°C was made because these are typical temperatures for InP substrate annealing and HES growth.

The composition of the solid solution and its lattice constant were determined by the RHEED method. The technique for measuring the composition and lattice constant is described in detail in [24,25,27]. The number of arsenic atoms in the InPAs and InAs solid solution was determined with dividing the volume of the InPAs and InAs islands solid solution by the unit cell volume of InAs. The volume of InAs islands was determined by the AFM method. Values of the lattice constant (a_0) of the InPAs solid solution and InAs islands are given in Table 3.

4. Experimental results

Data on the number of arsenic atoms (N_{As}) per 1 cm^2 in InPAs solid solution and InAs islands in case of cessation of annealing after structure formation (4×2) ($t = 0$ s) as well as after two minutes exposure in arsenic flux after structure formation (4×2) ($t = 120$ s) are presented in Table 4. For InPAs solid solution, data are presented only for $t = 0$ s, as no change in solid solution composition was detected during the two-minute exposure in arsenic flux [27]. The InPAs layer thickness, which was used to determine the number of arsenic atoms, was 1 nm [24], which correlates to the depth of penetration of the electron beam into the crystal at electron energy of 12 kV and angle of incidence $\sim 3°$, i.e. to the depth equal to approximately 1 nm [38].

Table 4 shows that the number of arsenic atoms at $t = 0$ s and at $t = 120$ s changes only in InAs islands. Therefore, by determining the difference in the number of arsenic atoms in InAs between $t = 0$ s and $t = 120$ s, divided by the exposure time in the arsenic flux and by the number of phosphorus atoms in one monolayer, we can determine what part of the phosphorus monolayer (k_P) desorbs per unit time from 1 cm^2. The dependence of k_P on T_{sub} is shown in Fig. 2. The activation energy of phosphorus desorption (E_a) was determined from approximation of k_P as a function $k_P = A \cdot \exp^{-(E_a/kT_{sub})}$, which was 2.7 ± 0.2 eV.

The activation energy of phosphorus desorption includes the energies of several elementary processes: the formation of the phosphorus atom due to the breaking of the chemical bond In-P and the migration of phosphorus over the terrace surface, as well as the evaporation of phosphorus atom into vacuum. The value of the energy of each elementary process depends on the experimental conditions. A change in the total pressure in the MOCVD reactor from 10

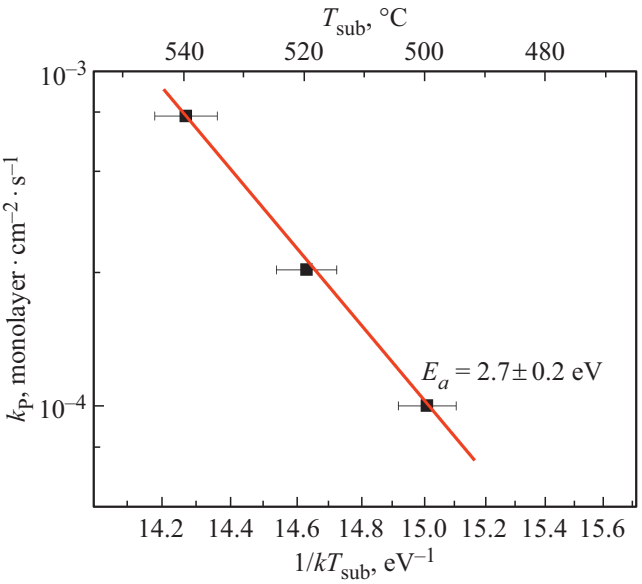

Figure 2. The number of phosphorus desorbing monolayers k_P per unit time from 1 cm^2.

to 5−20 kPa has been found to change the desorption rate [39]. The phosphorus dimers, which are observed on InP(001) surface with structure (2×2) at 10^{-2} Torr tributylphosphine pressure and temperature 530°C, also influence the phosphorus desorption rate [39,40]. Clearly, the near-surface layer of InPAs with InAs islands on InP(001) surface with (4×2) structure also influences the desorption rate of phosphorus. Therefore, it is not possible to directly compare the obtained value of the activation energy of phosphorus desorption with the literature data. An important application of the research presented here is to control the composition of $In_xGa_{1-x}As_yP_{1-y}$ films during MBE. These semiconductor solid solutions are often used in photonic devices [41,42]. They are difficult to grow because small changes in the amount of arsenic supplied to the growth chamber from molecular source produce to large changes in the atomic fraction of arsenic (y) in the film, since the growth temperature of such layers is higher than the desorption temperature of phosphorus. Knowledge of the desorbing phosphorus flow and its activation energy is important in determining film composition.

5. Conclusion

In this work, the process of phosphorus desorption from *epi-ready* InP(001) substrates during high-temperature annealing in an arsenic flux is studied experimentally. The original methodology is proposed for determining the number of phosphorus atoms desorbing from the surface. InPAs solid solution and InAs islands are formed on the surface during annealing, and indium atoms which arrive at the surface by breaking the bond with phosphorus atoms take part in the formation of it. The number of Indium atoms breaking the bond with phosphorus was determined from the change in the number of arsenic atoms between the samples annealed when the structure was formed (4×2) and additionally exposed to an arsenic flux for 2 minutes after structure formation (4×2), and consequently, the flow of phosphorus desorbing from the surface was determined. The flow of phosphorus desorbing from the surface increases from $1 \cdot 10^{-4}$ monolayer $\cdot$ cm$^2 \cdot$ s^{-1} at annealing temperature of 500°C to $7.3 \cdot 10^{-4}$ monolayer $\cdot$ cm$^2 \cdot$ s^{-1} at 540°C. The activation energy of the phosphorus desorption process was 2.7 ± 0.2 eV.

Funding

The study has been performed under the state assignment of ISP SB RAS.

Conflict of interest

The authors declare that they have no conflict of interest.

References

[1] S. Lee, M. Winslow, C.H. Grein, S.H. Kodati, A.H. Jones, D.R. Fink, P. Das, M.M. Hayat, T.J. Ronningen, J.C. Campbell, S. Krishna. Sci. Rep., **10**, 16735 (2020).
[2] J.A. del Alamo. Nature, **479**, 317 (2011).
[3] W.C. Huang, C.T. Horng. Appl. Surf. Sci., **257**, 3565 (2011).
[4] H. Yoo, K.S. Lee, S. Nahm, G.W. Hwang, S. Kim. Appl. Surf. Sci., **578**, 151972 (2022).
[5] R. Nagarajan, M. Kato, J. Pleumeekers, P. Evans, S. Corzine, S. Hurtt, A. Dentai, S. Myrthy, M. Missey, R. Muthiah, R. Salvatore, C. Joyner, R. Schneider, M. Ziari, F. Kish, D. Welch. IEEE J. Select. Topics Quant. Electron., **16**, 1119 (2010).
[6] K.S. Zhuravlev, A.L. Chizh, K.B. Mikitchuk, A.M. Gilinsky, I.B. Chistokhin, N.A. Valisheva, D.V. Dmitriev, A.I. Toropov, M.S. Aksenov. J. Semicond., **43**, 012302 (2022).
[7] D.V. Dmitriev, N.A. Valisheva, A.M. Gilinsky, I.B. Chistokhin, A.I. Toropov, K.S. Zhuravlev. IOP Conf. Ser.: Mater. Sci. Eng., **475**, 012022 (2019).
[8] D.V. Dmitriev, D.A. Kolosovsky, A.I. Toropov, K.S. Zhuravlev. Avtometriya, **57** (5), 1 (2021) (in Russian).
[9] R. Averbeck, H. Riechert, H. Schlotterer. Appl. Phys. Lett., **59**, 1732 (1991).
[10] S. Kanjanachuchai, T. Wongpinij, C. Euaruksakul, P. Photongkam. Appl. Surf. Sci., **542**, 148549 (2021).
[11] C.H. Li, L. Li, D.C. Law, S.B. Visbeck, R.F. Hicks. Phys. Rev. B, **65**, 205322 (2002).
[12] G.J. Davies, R. Heckingbottom, H. Ohno, C.E.C. Wood, A.R. Calawa, Appl. Phys. Lett., **37**, 290 (1980).
[13] S.L. Zuo, W.G. Bi, C.W. Tu, E.T. Yu. J. Vac. Sci. Technol. B, **16**, 2395 (1998).
[14] A. Chen, E. Murphy. *Broadband optical modulators: Science, Technology, and Applications* (Boca Raton, CRC Press, 2012).
[15] H. Ikeda, Y. Miura, N. Takahashi, A. Koukitu, H. Seki. Appl. Surf. Sci., **82**, 257 (1994).
[16] Z. Sobiesierski, D.I. Westwood, P.J. Parbrook, K.B. Ozanyan, M. Hopkinson, C.R. Whitehouse. Appl. Phys. Lett., **70**, 1423 (1997).
[17] N. Kobayashi, Y. Kobayashi. J. Cryst. Growth, **124**, 525 (1992).
[18] J.M. Moison, M. Bensoussan, F. Houzay. Phys. Rev. B, **34** (3), 2018 (1986).
[19] G. Hollinger, D. Gallet, M. Gendry, C. Santinelli, P. Viktorovitch. J. Vac. Sci. Technol. B, **8**, 832 (1990).
[20] J.M. Moison, C. Guille, M. Van Rompay, F. Barthe, F. Houzay, M. Bensoussan. Phys. Rev. B, **39**, 1772 (1989).
[21] T.W. Lee, H. Hwang, Y. Moon, E. Yoon. J. Vac. Sci. Technol. A, **17**, 2663 (1999).
[22] N. Kobayashi, Y. Kobayashi. Jpn. J. Appl. Phys. Pt **2**, **30**, L1699 (1991).
[23] Y. Sun, D.C. Law, S.B. Visbeck, R.F. Hicks. Surf. Sci., **513**, 256 (2002).
[24] D.V. Dmitriev, D.A. Kolosovsky, T.A. Gavrilova, A.K. Gutakovskii, A.I. Toropov, K.S. Zhuravlev. Surf. Sci., **710**, 121861 (2021).
[25] D.V. Dmitriev, I.A. Mitrofanov, D.A. Kolosovsky, A.I. Toropov, K.S. Zhuravlev. 21st Int. Conf. Young Specialists on Micro/Nanotechnologies and Electron Devices (EDM), 5 (2020).

[26] D. Kolosovsky, D. Dmitriev, T. Gavrilova, A. Toropov, A. Kozhukhov, K. Zhuravlev. IEEE 22nd Int. Conf. Young Professionals in Electron Devices and Materials (EDM), 17 (2021).
[27] D.V. Dmitriev, D.A. Kolosovsky, E.V. Fedosenko, A.I. Toropov, K.S. Zhuravlev. FTP, **55** (10), 877 (2021) (in Russian).
[28] G. Hollinger, E. Bergignat, J. Joseph, Y. Robach. J. Vac. Sci. Technol. A, **3**, 2082 (1985).
[29] Y.S. Lee, W.A. Anderson. J. Appl. Phys., **65** (10), 4051 (1989).
[30] A. Nelson, K. Geib, C.W. Wilmsen. J. Appl. Phys., **54** (7), 4134 (1983).
[31] N. Shibata, H. Ikoma. Jpn. J. Appl. Phys., **31** (12R), 3976 (1992).
[32] M.B. Panish, J.R. Arthur. J. Chem. Therm., **2** (3), 299 (1970).
[33] J.R. Arthur. J. Phys. Chem. Sol., **28** (11), 2257 (1967).
[34] H. Seki, A. Koukitli. J. Cryst. Growth, **78** (2), 342 (1986).
[35] S. Katsura, Y. Sugiyama, O. Oda, M. Tacano. Appl. Phys. Lett., **62**, 1910 (1993).
[36] Q.-K. Xue, T. Hashizume, T. Sakurai. Progr. Surf. Sci., **56**, 1 (1997).
[37] A.Y. Cho, J.C. Tracy. US Patent № 3,969,164.
[38] H. Yamaguchi, Y. Horikoshi. Phys. Rev. B, **44**, 5897 (1991).
[39] O. Feron, M. Sugiyama, W. Asawamethapant, N. Futakuchi, Y. Feurprier, Y. Nakano, Y. Shimogaki. Appl. Surf. Sci., **157**, 318 (2000).
[40] L. Li, B.-K. Han, D. Law, C.H. Li, Q. Fu, R.F. Hicks. Appl. Phys. Lett., **75**, 683 (1999).
[41] D. Yap, K.R. Elliott, Y.K. Brown, A.R. Kost, E.S. Ponti. IEEE Phot. Techn. Lett., **13**, 26 (2001).
[42] H. Takeuchi, K. Tsuzuki, K. Sato, M. Yamamoto, Y. Itaya, A. Sano, M. Yoneyama, T. Otsuji. IEEE J. Select. Topics Quant. Electron., **3**, 336 (1997).